

LASER INTERFEROMETER GRAVITATIONAL WAVE OBSERVATORY  
- LIGO -  
CALIFORNIA INSTITUTE OF TECHNOLOGY  
MASSACHUSETTS INSTITUTE OF TECHNOLOGY

LIGO-XXXXXXX-XX-X Date: 2009/09/25

**Multiply Resonant EOM for the  
LIGO 40-meter Interferometer**

Stephanie Erickson  
Mentor: Rana Adhikari, Koji Arai

**California Institute of Technology**  
**LIGO Project, MS 18-34**  
**Pasadena, CA 91125**  
Phone (626) 395-2129  
Fax (626) 304-9834  
E-mail: info@ligo.caltech.edu

**Massachusetts Institute of Technology**  
**LIGO Project, Room NW22-295**  
**Cambridge, MA 02139**  
Phone (617) 253-4824  
Fax (617) 253-7014  
E-mail: info@ligo.mit.edu

**LIGO Hanford Observatory**  
**Route 10, Mile Marker 2**  
**Richland, WA 99352**  
Phone (509) 372-8106  
Fax (509) 372-8137  
E-mail: info@ligo.caltech.edu

**LIGO Livingston Observatory**  
**19100 LIGO Lane**  
**Livingston, LA 70754**  
Phone (225) 686-3100  
Fax (225) 686-7189  
E-mail: info@ligo.caltech.edu

<http://www.ligo.caltech.edu/>

**Abstract**

The Laser Interferometer Gravitational-Wave Observatory (LIGO) uses a Michelson interferometer with Fabry-Perot cavities to sense strains induced by gravitational waves. Length sensing and control is achieved through locking the optical cavity lengths to the laser wavelength. For locking, an electro-optic modulator (EOM) is utilized to modulate the phase, creating frequency sidebands. For the upgrade of the 40-meter prototype interferometer, used to test systems before implementation in the full-scale observatories, there will be three modulation frequencies: 11 and 55, and 29.5 MHz, used for control of the mirrors in the main interferometer and mode cleaner, respectively. The purpose of this project was to design, build and test a triply resonant circuit for the 40-m upgrade, allowing three modulations to occur inside one EOM rather than several, reducing wavefront deformation, power loss, and problems with alignment. Resonance will allow for lower driving voltages and suppression of harmonics. The designed circuit has resonance at the necessary frequencies, with roughly equivalent gain and an impedance of  $50 \Omega$  at each peak. Several iterations of the circuit were built, and the performance of each was evaluated by measuring the transfer function and impedance, and by observing the sidebands using an optical spectrum analyzer.

# Contents

<b>1</b>	<b>Background and Motivation</b>	<b>3</b>
<b>2</b>	<b>Circuit Design</b>	<b>4</b>
2.1	Conceptual Design . . . . .	4
2.2	Specifications . . . . .	5
<b>3</b>	<b>Circuit Testing</b>	<b>6</b>
3.1	Flying-Component Circuit . . . . .	6
3.2	Impedance . . . . .	7
3.3	Optical Spectrum Analyzer . . . . .	10
<b>4</b>	<b>Suggestions for Future Work</b>	<b>11</b>
<b>5</b>	<b>Summary and Conclusion</b>	<b>12</b>
<b>A</b>	<b>Methods</b>	<b>12</b>
A.1	Impedance Measurement . . . . .	12
<b>B</b>	<b>Resources</b>	<b>14</b>
<b>C</b>	<b>Acknowledgements</b>	<b>14</b>

# 1 Background and Motivation

The Laser Interferometer Gravitational-Wave Observatory (LIGO) uses a Michelson interferometer with Fabry-Perot cavities to detect strains induced by gravitational waves. Fabry-Perot cavities use resonance to increase sensitivity to length displacements; to remain at resonance, the cavity's length must be an integer multiple of the wavelength of laser light used. To maintain the length for resonance, a feedback system is used; because the intensity will be the same on either side of resonance, modulation of the laser is used to distinguish between situations where the cavity length is too short and too long. This modulation is provided by an electro-optic modulator (EOM) [1, 2].

An EOM is an optical device that modulates the phase, polarization, or amplitude of light according to an electrical voltage signal. The indices of refraction of certain crystals are sensitive to electric fields; this property of a crystal can be exploited to create phase and polarization variations in light passed through the crystal (amplitude modulations are achieved by varying the polarization and passing the light through a polarizer). EOMs can be either resonant or broadband; a resonant EOM contains an LC circuit to create electrical resonance, which means that the input voltage can be much lower than the voltage across the crystal, while a broadband EOM does not contain this component and can be used to generate modulations of a wide range of frequencies. Resonant EOMs can only produce modulations at specific frequencies [3].

In LIGO, the EOM modulates the phase of the laser. Effectively, this phase modulation creates two frequency sidebands in the laser beam: one at the sum of the frequency of the laser light and the frequency of modulation, and one at the difference between them. As the modulated light enters a resonant cavity, a certain fraction of the light is reflected; this quantity depends on both the frequency of the incident beam and the length of the optical cavity. Because of this, it is possible to detect fluctuations in the cavity length as fluctuations in the power of the reflected light. Furthermore, through analysis of the relative power of the frequency components of the reflected beam, the direction of length displacement (too short or too long for resonance) can also be determined. To do this, the reflected power signal is mixed with the modulation signal to produce an error signal which is proportional to the displacement from resonance when the cavity length is close to resonance. This signal is used to drive a servo to control the length of the cavity, creating a feedback loop that keeps the cavity at resonance; since the signal represents the cavity length's deviation from resonance, it is also the signal with which gravitational waves will be detected. [1].

Currently, modulation is produced by two EOMs in a Mach-Zehnder interferometer configuration. The two main modulation frequencies are 33 and 166 MHz, and the mode cleaner modulation frequency is 29 MHz; since 29 MHz is close to 33 MHz, this modulation can be produced by driving the 33 MHz resonant EOM at the desired frequency. The Mach-Zehnder configuration increases the complexity of the setup, and its alignment affects the alignment going into the main interferometer. For the 40-m upgrade, the three modulations will occur in a single EOM, reducing the complexity that the Mach-Zehnder introduces [5]. Using fewer EOMs will also reduce wavefront distortion and power loss. While it would be possible to drive a broadband EOM at the three modulation frequencies, a resonant circuit will make it possible to drive the circuit with a low-amplitude voltage, while still maintaining a high voltage across the EOM. It also can provide suppression of the harmonics of the driving

frequencies.

For the 40-m upgrade, two sets of sidebands will be used for length and alignment sensing, and one set will be necessary to control the mode cleaner; therefore, three sets of sidebands must be created. This will be achieved by creating an EOM circuit with triple resonance. The goal of this project was to design, analyze, and test a triply resonant EOM for the upgrade of the 40-m prototype interferometer. This EOM may eventually be used to induce the three modulation frequencies necessary for locking and length sensing (GW detection) [4].

## 2 Circuit Design

### 2.1 Conceptual Design

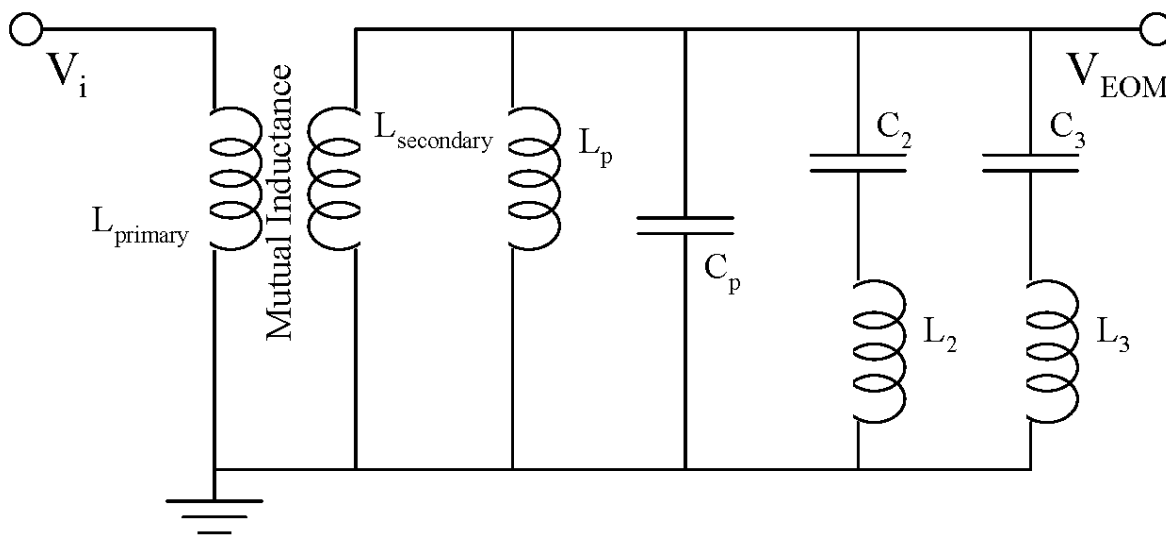


Figure 1: EOM circuit diagram

The basic conceptual design of the circuit is shown in Figure 1. First, a transformer is used to increase the voltage in the circuit; it does this by converting some power from current to voltage through mutual inductance. Next, the three resonant peaks must be introduced. Generally, the circuit creates the three necessary resonant peaks by creating one resonant peak, and two valleys within it. The inductance in the transformer and the inductor parallel to it, along with the EOM, which acts like a capacitor, and the capacitor in parallel with it, create a resonant peak, as shown in blue in Figure 2. This occurs because the energy in the circuit is transferred back and forth between the capacitances and the inductances with almost no energy loss, causing the oscillation to have a high amplitude.

The two inductor-capacitor pairs in parallel with these components create minima at two different frequencies, as shown in red in Figure 2. This occurs because, as the frequency approaches resonance, the impedance of the inductor-capacitor pair drops to zero, causing the

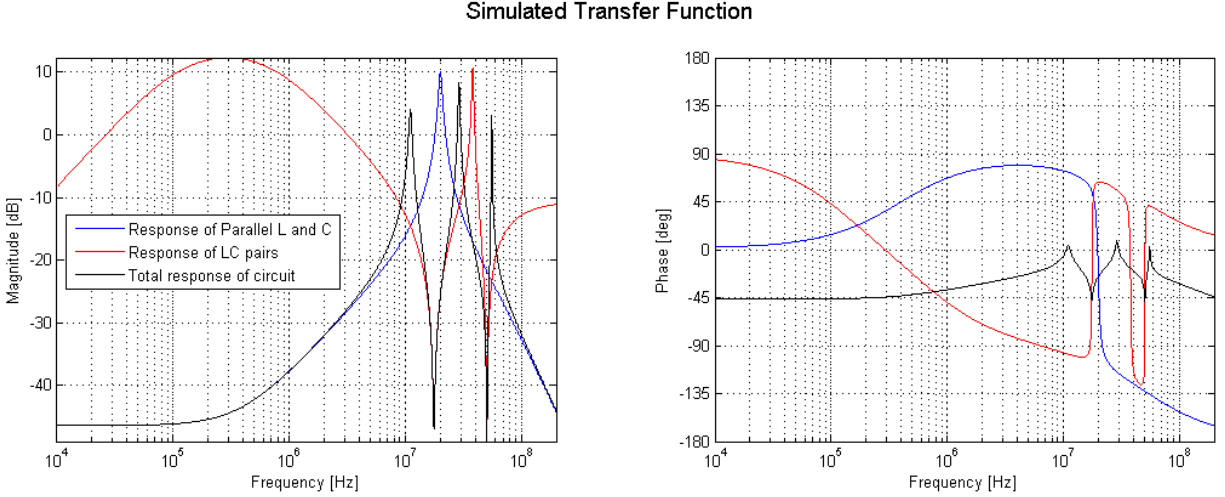


Figure 2: Theoretical performance of conceptual circuit

voltage across the pair to drop to zero as well. Although the voltage across each component is large, the two voltages combine to exactly cancel out. When the effect of these components are combined, the response of the circuit results. The overall response of the circuit is shown in black in Figure 2. The frequency placement of the resonant peaks is manipulated by changing the inductor and capacitor values and thereby changing the placement of the main peak and two valleys. The placement of the main peak and valleys can be calculated using the usual resonance relation, shown in the following equation.

$$\omega = \frac{1}{\sqrt{LC}} \quad (1)$$

However, the equation for calculating the location of each peak is more complicated; the best method for finding optimal component values seems to be trial-and-error, using circuit simulation software such as LTSpice or the transfer function of the circuit.

Resistors can also be added to achieve the desired input impedance. It is important for the input impedance to be the same as the source impedance for maximum power transfer; unequal impedance could also cause power reflection, which could distort the signal to the EOM. Adding a resistor in series with each LC pair makes it possible to adjust the impedance of each peak slightly more independently than if a single resistor were simply added at the input of the circuit. This make the impedance more adjustable.

## 2.2 Specifications

For functioning in the advanced-LIGO length-sensing scheme, the EOM circuit must meet a few specifications. For the 40-m upgrade, the circuit must have resonant frequencies of 11 MHz, 29.5 MHz, and 55 MHz, so that the EOM will modulate the phase of the laser at those frequencies. The 29.5 MHz frequency will be used to control the mode cleaner, while the other two will be used for length sensing in the main interferometer. The EOM used will be a New Focus EOM KTP 4064, which has a phase-modulation depth of 13 mrad/V;

since the optical modulation depth needs to be around 0.1 rad, the voltage across the EOM will need to be around 8.5 V at the 11 MHz and 55 MHz resonances. Since the maximum available power for a Marconi signal generator is 13 dBm, the circuit will need to provide a minimum gain of 15.7 dB. In addition to this, the impedance at each resonant frequency will need to be  $50 \Omega$  to avoid signal reflection into the oscillator. The voltage across the EOM should also be roughly equivalent at 11 MHz and 55 MHz [4].

## 3 Circuit Testing

### 3.1 Flying-Component Circuit

While flying-component circuits are not ideal for RF applications, it was decided that, since the relevant frequencies are below 100 MHz, a flying-component circuit could be used. This reduced the problems that can occur involving the electrostatic field of a board when using surface mount components. A flying-component version of the circuit was built according to the circuit diagram in Figure 3. A picture of the circuit is shown in Figure 4.

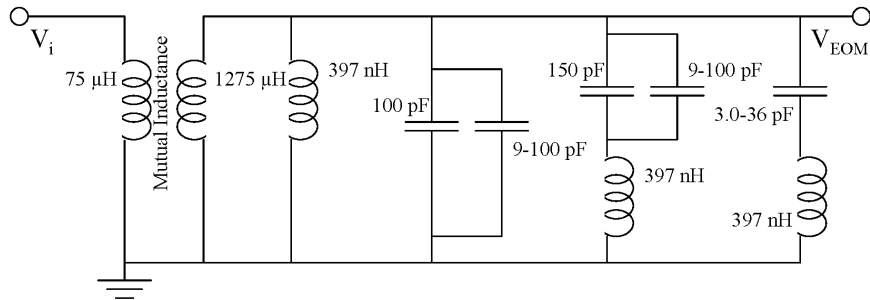


Figure 3: Circuit diagram of flying-component circuit

Next, the transfer function of the circuit was measured; the measured and simulated transfer functions are shown in Figure 5. As can be observed from the figure, the measured and simulated transfer functions were close to identical.

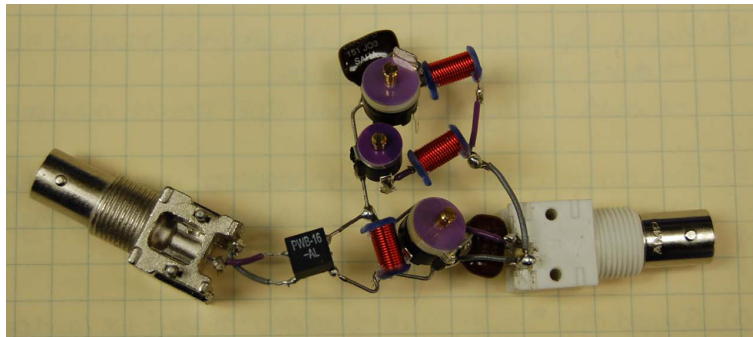


Figure 4: Picture of initial flying-component circuit

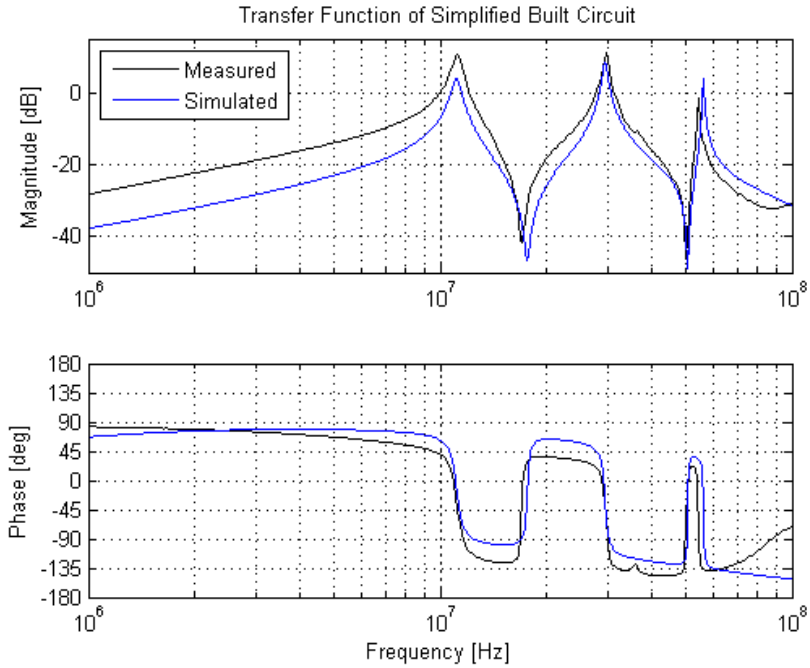


Figure 5: Measured and simulated transfer functions of flying-component circuit

### 3.2 Impedance

Once it was determined that the transfer function of the circuit was functioning properly, it was necessary to measure the input impedance of the circuit to ensure that it was close to  $50 \Omega$  at the resonant peaks to prevent power reflection when the circuit is driven at those frequencies. The original impedance measurement is shown in Figure 6.

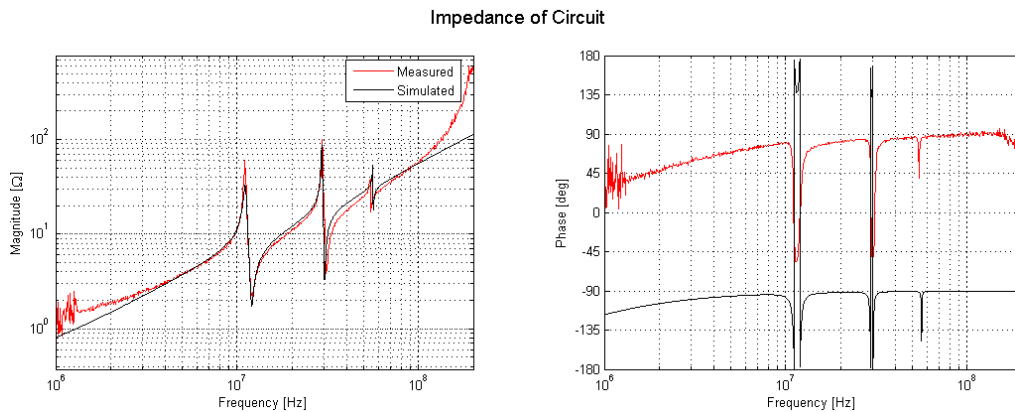


Figure 6: Initial impedance measurement shown with the expected impedance

After the original measurement was taken, a capacitor was added to simulate the behavior of the circuit while attached to the EOM. The impedance was then adjusted using resistors until the impedance was at least the same order of magnitude as  $50 \Omega$ . Once this was done,

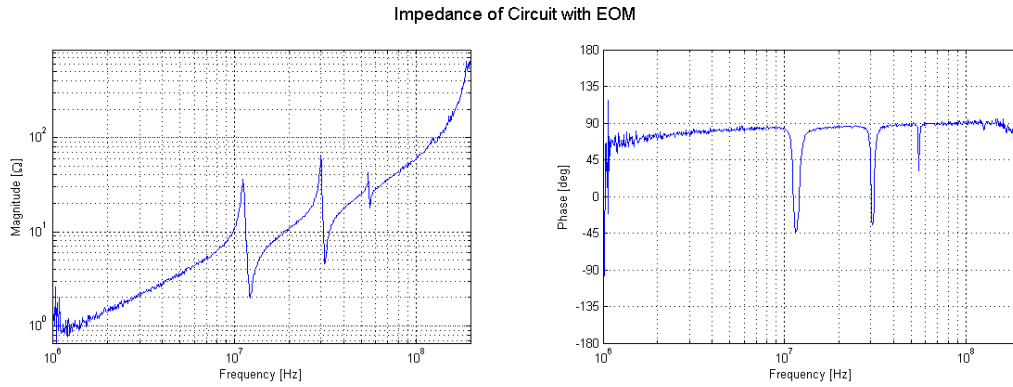


Figure 7: Impedance measurement of circuit attached to EOM

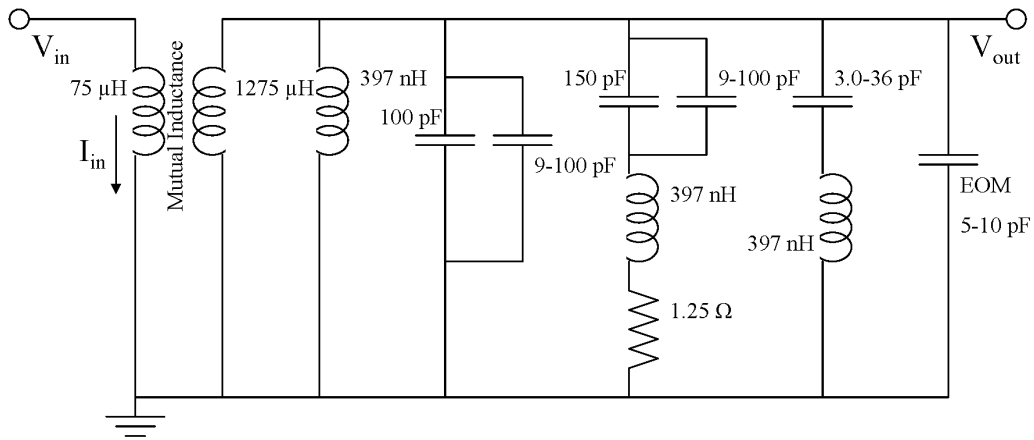


Figure 8: Circuit diagram for final flying-component circuit

the capacitor was removed, and the circuit was attached to the EOM; the impedance of this new setup was then measured. The final impedance of this circuit is shown in Figure 7. A circuit diagram showing the flying-component circuit attached to the EOM is shown in Figure 8. Pictures of the circuit are shown in Figures 9 and 10.



Figure 9: Picture of flying-component circuit in box attached to EOM

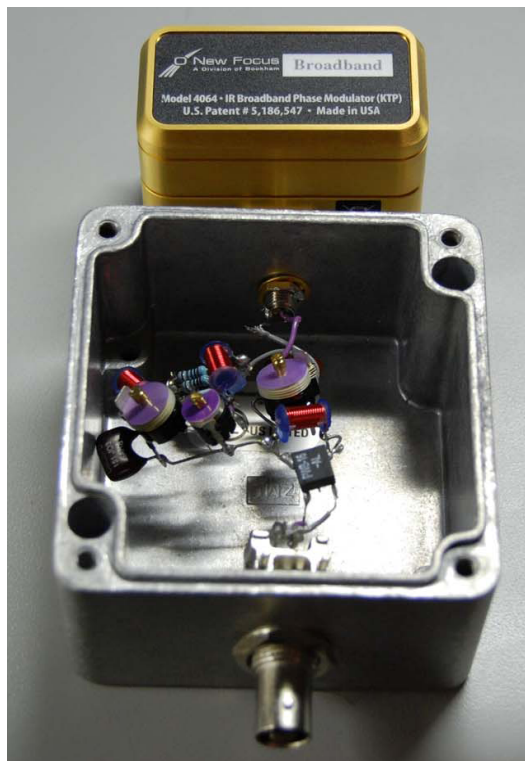


Figure 10: Another angle of circuit in box

### 3.3 Optical Spectrum Analyzer

Next, the circuit was tested using an optical spectrum analyzer. The optical spectrum analyzer contains a scanning Fabry-Perot cavity; when the resonant frequency of the cavity is equal to the frequency of the laser, light is transmitted through the cavity to a photodetector. One of the mirrors is displaced using a piezoelectric mirror spacer driven by an oscillating voltage signal, thereby varying the resonant frequency of the cavity, and the frequency of light transmitted to the photodetector. Through this process, the intensity of light at each frequency can be determined and the spectral makeup of the beam can be analyzed. A diagram illustrating the setup for this test is shown in Figure 11. For this circuit, it was necessary to use an RF amplifier with a gain of around 27 dB to increase the signal from the signal generator so that the modulation of the beam could be observed.

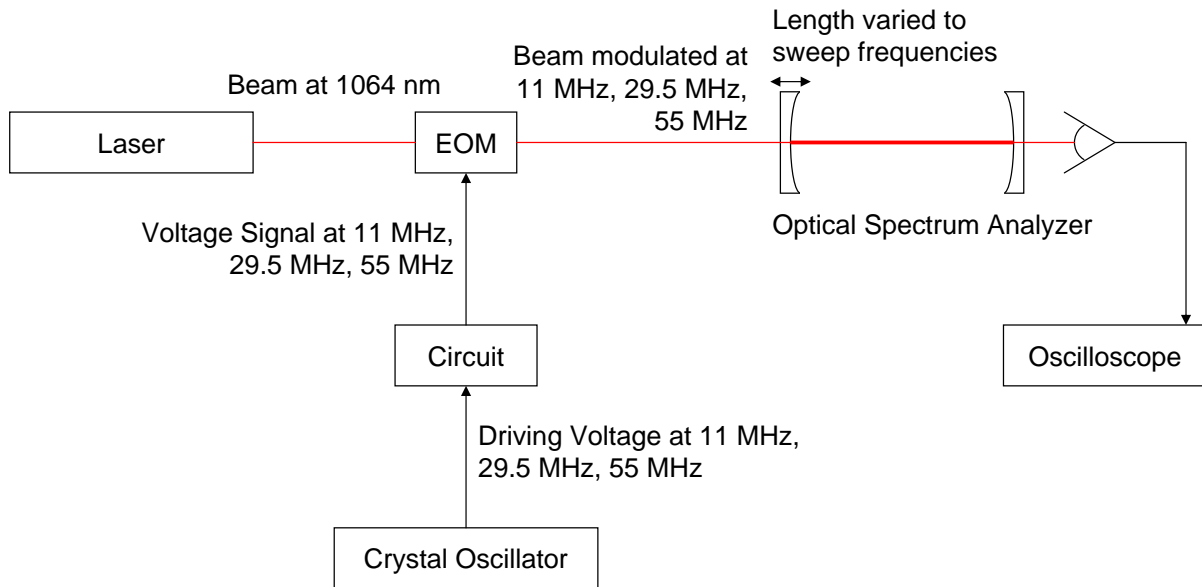


Figure 11: Optical spectrum analyzer setup

The optical spectrum analyzer setup was used to measure several different aspects of the modulation resulting from the circuit. First, the modulation depth at different frequencies was measured. This was done by measuring the ratio between the height of the sideband peak and the height of the carrier peak on the oscilloscope. The modulation depth could then be calculated from that value using the following equation:

$$m \approx \sqrt{\frac{4R}{1 + 2R}} \quad (2)$$

where  $R$  is the ratio and  $m$  is the modulation depth. These values were then divided by the voltage across the input terminals of the circuit to create the results shown in Figure 12.

The measured and expected plots look similar, although the measured values appear to be higher for both the 29.5 and 55 MHz peaks. Ideally, for the two to be compared, the transfer function of the circuit would be measured across the plates inside the EOM; since it was

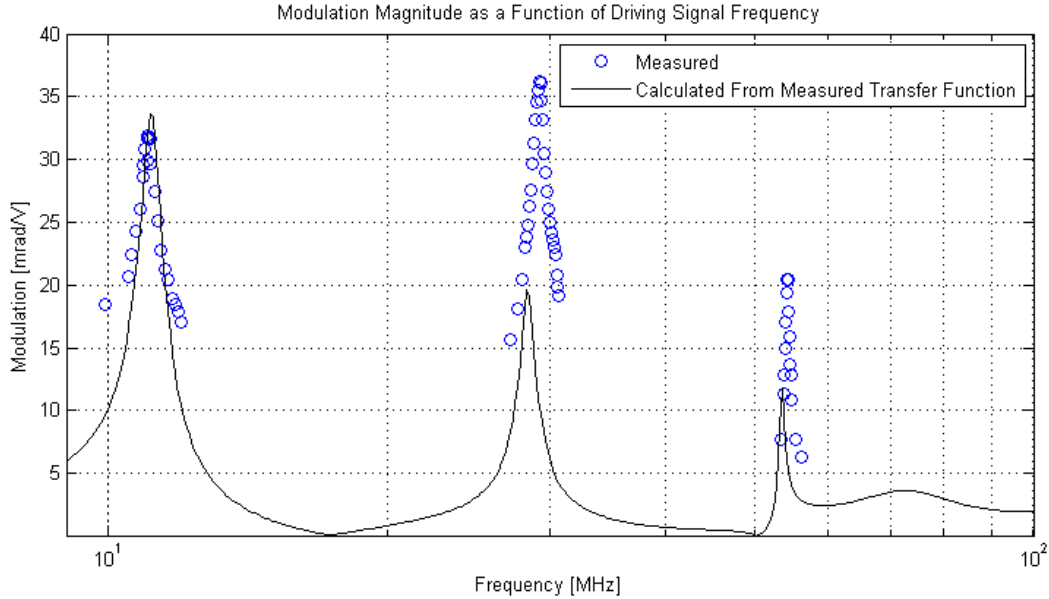


Figure 12: Measured modulation depth as a function of frequency, shown with the expected modulation depth as calculated using the measured transfer function and the nominal modulation depth of the commercially purchased EOM (13 mrad/V)

impossible to do that, any discrepancies between the two sets of data are likely due to the different measuring points. In addition to this, it was discovered that the peaks were at 11.11, 29.57, and 54.70 MHz; although these are not at the exact desired frequencies, those frequencies could likely be reached through careful tuning.

Next, the linear dependance of modulation depth on the voltage at the input of the circuit was quantified at each resonant peak to determine whether voltage could be adjusted linearly to produce the desired modulation depth. The results of this measurement are shown in Figure 13.

In each plot, there are two sets of data; these correspond to the sidebands on either side of the carrier beam. Especially in the 11.11 MHz peak, the data from the sidebands are separated; this is due to an asymmetry in the carrier beam that appeared to distort the close sidebands. In fact, the second sideband was not even visible for at low input voltages because it was masked by the edge of the carrier peak. Overall, the results look relatively linear; it appears that varying the voltage would cause a proportional variation in the modulation depth. This property is useful, because it allows for easy control over the modulation depth produced by the EOM.

## 4 Suggestions for Future Work

The modulation depth is not equivalent for all three sidebands; the 55 MHz peak is lower than the other two, while the 29.5 MHz peak is relatively high. Ideally, the 11 MHz and 55 MHz peaks would be approximately equivalent, while the 29.5 MHz peak could be much

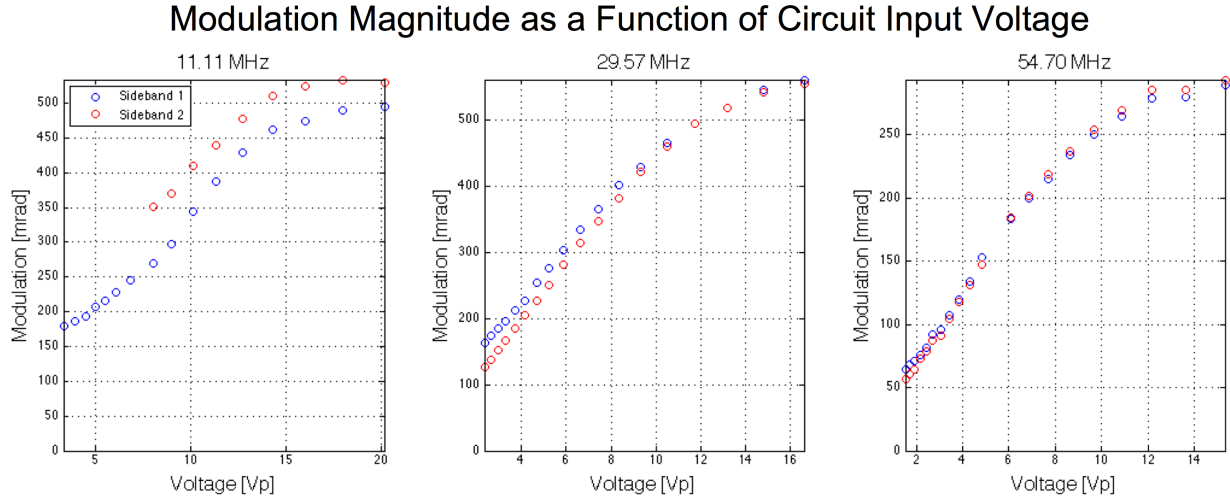


Figure 13: Linear dependance of modulation depth on voltage across input terminals of circuit at each resonant peak (11.11, 29.57, 54.70 MHz)

lower. Future work on this project would attempt to correct this imbalance in the modulation depth at the resonant peaks.

## 5 Summary and Conclusion

A triply resonant circuit was created and attached to a commercially available EOM in order to modulate the phase of a laser beam at three frequencies. The transfer function and impedance of the circuit were first tested, and it was confirmed that the circuit performed roughly as expected, with peaks in gain and an impedance of  $50\ \Omega$  at roughly 11, 29.5, and 55 MHz. Although the gain of the circuit is not as specified, it was possible to use an RF amplifier to increase the gain and produce the desired outcome. The circuit was then attached to an EOM, and a laser beam was modulated; the modulation depth due to the circuit was then quantified and compared to the expected response. The actual resonant frequencies were measured to be 11.11, 29.57, and 54.70 MHz. The linearity at each resonant peak was then observed to ensure that variations in the input voltage would result in proportional variations in the resulting modulation depth. Although this circuit does not work exactly as specified at this point in time, it was demonstrated that a triply resonant passive circuit in conjunction with an RF amplifier could be used to create the necessary frequency sidebands.

## A Methods

### A.1 Impedance Measurement

An impedance measurement was made using the Agilent 4395A Network Analyzer. This was done by attaching both the A and R ports to the input terminals of the circuit and measuring the transfer function between them. If the network analyzer were ideal, this measurement

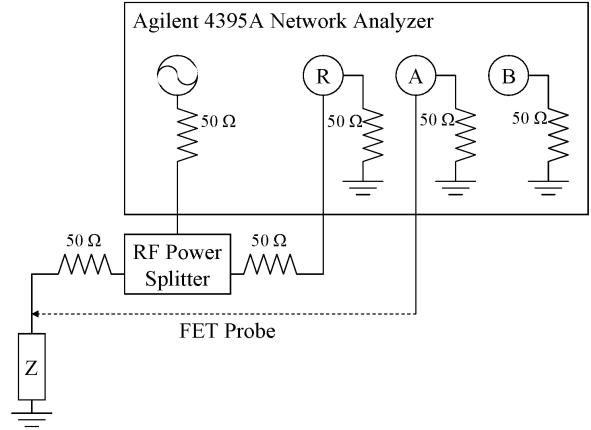


Figure 14: Schematic of impedance testing setup

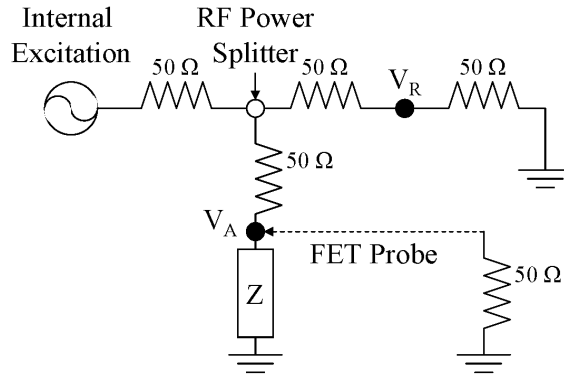


Figure 15: Circuit diagram showing the behavior of the impedance testing setup

would simply yield a transfer function of 1 (0 dB) for all frequencies; however, the electrical setup of the analyzer looks more like the diagram shown in Figure 14. For analysis purposes; the power splitter can be treated as a simple node, and the setup simplifies to the following circuit diagram (Figure 15). From this figure, it is possible to calculate that the transfer function is described by the following equation:

$$\frac{V_A}{V_R} = \frac{2Z}{Z + 50} \quad (3)$$

where Z is the impedance of the component being tested. In practice, attenuators must be used to prevent signal reflection back into the power splitter. A diagram of the actual setup is shown in Figure 16.

The system was then calibrated using a 50-Ω BNC termination, since the transfer function for that impedance should be 1 (0 dB) at all frequencies. Once the system was calibrated, and several impedances were tested to demonstrate that the system was functioning roughly as expected, the impedance of the circuit was measured.

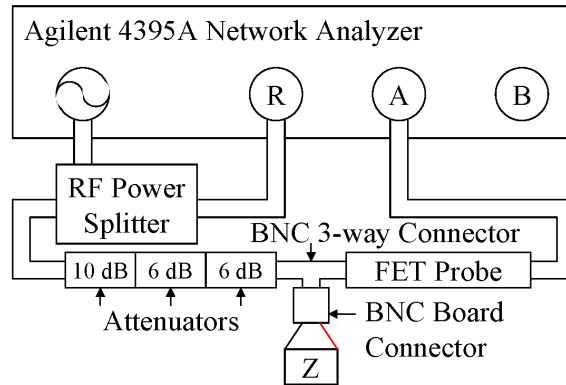


Figure 16: Schematic showing actual setup of Agilent 4395A for impedance testing

## B Resources

- [1] Black, E. (1998). Notes on the Pound-Drever-Hall technique. *LIGO Project*. Pasadena, CA: California Institute of Technology and Cambridge, MA: Massachusetts Institute of Technology. Retrieved May 11, 2009 from <http://www.ligo.caltech.edu/docs/T/T980045-00.pdf>
- [2] Paschotta, R. (2008). Stabilization of Lasers. *Encyclopedia of Laser Physics and Technology*. RP Photonics. Retrieved May 10, 2009 from [http://www.rp-photonics.com/stabilization\\_of\\_lasers.html](http://www.rp-photonics.com/stabilization_of_lasers.html)
- [3] Paschotta, R. (2008). Electro-optic Modulators. *Encyclopedia of Laser Physics and Technology*. RP Photonics. Retrieved May 10, 2009 from [http://www.rp-photonics.com/electro\\_optic\\_modulators.html](http://www.rp-photonics.com/electro_optic_modulators.html)
- [4] Multiply Resonant EOM. *40m wiki*. Pasadena, CA: California Institute of Technology, LIGO Labs. Retrieved April 17, 2009 from [http://lhocds.ligo-wa.caltech.edu:8000/40m/Multiply\\_Resonant\\_EOM](http://lhocds.ligo-wa.caltech.edu:8000/40m/Multiply_Resonant_EOM)
- [5] Miyakawa, O., Kawamura, S., Barr, B., & Vass, S. (2004). Mach-Zehnder interferometer for Advanced-LIGO optical configurations to eliminate sidebands of sidebands. *LIGO Project*. Pasadena, CA: California Institute of Technology and Cambridge, MA: Massachusetts Institute of Technology. Retrieved August 3, 2009 from <http://www.ligo.caltech.edu/docs/T/T040119-00.pdf>

## C Acknowledgements

Mentors: Rana Adhikari, Koji Arai  
 Other Help: Alberto Stochino  
 LIGO 40-m Lab  
 Caltech SURF Program  
 National Science Foundation